International Journal of Energy Production and Management
Vol. 9, No. 2, June, 2024, pp. 113-120
Journal homepage: http://iieta.org/journals/ijepm

A Study on the Effect of Cellulose Nanocrystalline Paper on PVA-KOH Electrolyte Membranes for Increasing Ionic Conductivity

Firman Ridwan*, Nanda Febriyan, Muhammad Akbar Husin, Faris Aulia

Department of Mechanical Engineering, Universitas Andalas, West Sumatera 25175, Indonesia

Corresponding Author Email: firmanridwan@eng.unand.ac.id

https://doi.org/10.18280/ijepm.090206

Received: 8 March 2024
Revised: 3 June 2024
Accepted: 20 June 2024
Available online: 30 June 2024

Keywords:
NCC, composite, ionic conductivity, tensile strength, power density

ABSTRACT

The enhancement of ionic conductivity and tensile strength in electrolyte membranes by nanoparticles is a key factor driving increased interest in their use. Increasing conductive and strong membranes has the same meaning for energy storage. Conductive solid electrolyte membranes are made by mixing Potassium Hydroxide (KOH), Polyvinyl Alcohol (PVA), and Glycerol with the addition of nanocrystalline cellulose (NCC) paper. Paper NCC is made using the hydrolysis method. In this study, an increase in conductivity and tensile strength due to differences in NCC composition with variations of 0 g, 1 g, 3 g, and 5 g in the electrolyte membrane was observed. The test results show that the highest conductivity of 0.0512 $S.cm^{-1}$ was obtained from 3 g NCC according to the membrane test results. The addition of NCC weighing 5 g resulted in the highest tensile strength, namely 6.91 MPa. Furthermore, the addition of 5 g of NCC resulted in the largest energy production of 0.000188 W/cm^2. The inclusion of NCC in the PVA-KOH membrane was found to increase the tensile strength and ionic conductivity of the electrolyte membrane. The results show that the incorporation of NCC increases the conductivity and strength of the membrane, thereby showing its potential for use in the future development of aluminum air batteries.

1. INTRODUCTION

The escalation in energy demand and the pursuit of renewable sources have led to the growing importance of energy usage. Consequently, there has been notable curiosity regarding the application of nanoparticles in electrolyte membranes to improve their ionic conductivity. This underscore efforts directed towards the development of more efficient and sustainable energy storage technology. The crucial importance of creating electrolyte membranes with elevated ionic conductivity must not be underestimated, particularly in the realm of propelling energy storage technologies like fuel cells and batteries. Prior studies have demonstrated that the incorporation of nanoparticles in PVA-based solid polymer electrolytes with KOH additives can boost their ionic conductivity. Further investigation is necessary to establish the influence of diverse nanoparticle concentrations on membrane conductivity. Given the lack of a thorough understanding regarding the most effective concentration of nanoparticles necessary to achieve the highest ionic conductivity in PVA based solid polymer electrolytes. Solid Polymer Electrolytes (SPE) possess numerous benefits compared to liquid electrolytes within the scope of aluminum-air batteries.

SPE is renowned for its superior electrochemical and thermal stability, impermeable attributes, and enhanced safety, particularly in wearable electrochemical devices [1]. PVA exhibits a notable resistance to the proliferation of organisms such as algae and fungi [2]. The integration of PVA-based membranes is of utmost importance in various applications like pervaporation, reverse osmosis desalination, CO_2 separation, and ion exchange, and thus calls for meticulous attention to detail [3]. This is attributed to the formation of a porous structure resulting from the aggregation of PVA chains in solvents with low polarity [4, 5]. The electrolyte membrane made of PVA demonstrates improved proton conductivity and resistance to methanol cross-linking, making PVA a multifaceted material with promising potential in areas such as network engineering, food packaging, and smoke filtration [6].

Nanocrystalline cellulose is a type of nano cellulose made from natural cellulose and has high crystallinity and a very fine nano network structure [7]. The investigation unveiled that the introduction of NCC enhanced the mechanical characteristics of PVA membranes, which encompass the augmentation of tensile strength and modulus. Additionally, NCC heightens the thermal stability of the membranes. The inquiry ascertained that the integration of NCC in PVA membranes presents a promising strategy to ameliorate their mechanical and thermal properties [8]. Furthermore, incorporating NCC may lead to improved ionic conductivity of PVA membranes. The presence of NCC within the membranes establishes a structural framework, which in turn facilitates the movement of ions and elevates the overall conductivity. Furthermore, the introduction of NCC at a concentration of 3% by weight can

yield improvements in the mechanical properties, as documented in the literature [9]. Paper is an affordable and suitable option for NCC, providing effective cost and nanocrystal sustainable production [10]. The enhancement of ionic conductivity in electrolyte membranes through NCC has been proven [11–13]. NCC leads to better functionality in fuel cells and other electrochemical devices [14]. It has been discovered that NCC fusion enhances membrane permeability and selectivity [15]. Nanocellulose, particularly nanocrystalline cellulose (NCC), has the potential to be integrated into electrolyte membranes in order to enhance their characteristics [16]. The inclusion of NCC in the polymer matrix can markedly enhance the mechanical properties of the membrane, rendering it more robust and impervious to harm. This is particularly critical in fuel cell applications, wherein the membrane necessitates the ability to endure demanding operating conditions [17]. Lower concentrations of NCC are more favorable for producing optimal membrane properties, whereas higher concentrations may lead to the aggregation and defects in the membrane structure [18]. The impact of introducing KOH into the membrane as an electrolyte has been empirically demonstrated to have a substantial influence on its properties. This augmentation in conductivity can be ascribed to the augmentation in the quantity of ions available as a result of ion dissociation. The existence of KOH as an ionic dopant encourages the creation of freely mobile ions, thereby instigating heightened conductivity in the electrolyte [19]. When combined, PVA and NCC with KOH engender a composite electrolyte membrane. Composite alkaline polymer electrolytes manifest augmented ionic conductivity at ambient temperatures [20]. Plasticizers can enhance the flexibility of a polymer by being incorporated into its composition. Polymer electrolytes electrical conductivity can be raised by adding plasticizers [21]. Glycerol is one of the plasticizers utilized. Glycerol is an adaptable substance that can be utilized to enhance the qualities of polymers like PVA by acting as a plasticizer. The effects include lowering the melting temperature, establishing hydrogen bonds with the polymer, and improving the workability and flexibility of biopolymer-based membranes. Similar mechanical, optical, and barrier properties are shared by membranes made with varying glycerol purities. Plasticization costs can be lowered by up to six times using glycerol [22]. Despite glycerol having numerous beneficial uses, it also possesses several drawbacks. One of the primary challenges associated with the item is its inherent volatility, which can restrict its utility in certain situations Glycerol can be utilized as a plasticizer for PVA in specific applications [23].

In summary, there is a lot of potential for using PVA-based membranes with the right modifications in a variety of applications, from separation technology to the creation of cutting-edge products across multiple industries. The enhanced proton conductivity and durability of PVA present new possibilities for the creation of high-performance, eco-friendly materials. The aim of this study is to determine the impact of different amounts of nanocrystalline paper on the ionic conductivity of the membrane.

2. METHODS

2.1 Materials

The chemicals used in this study include PVA, KOH, NaOH, NaClO, H_2SO_4, and Glycerol, all from Merck. Ensuring high purity is crucial, especially for chemical synthesis and electrochemical applications.

2.2 Characterization

2.2.1 Scanning Electron Microscopy (SEM)

Scanning Electron Microscopy (SEM) is highly versatile characterization of 2D and 3D materials with high spatial resolution, complementary to nondestructive techniques from nano to microscale in both imaging and chemical characterization modes [24]. SEM was conducted using the Hitachi S-3400N instrument to investigate the morphology, particle size, and membrane characteristic coupling of the biomaterial composite. SEM have a magnification range from 5 to 300,000 times, an accelerating voltage ranging from 300V to 30kV, and ultra-high resolution of 5120 x 3840. In the context of SEM, it is noted that several sample components are embedded on a metal substrate. The Hitachi S-3400N instrument enables precise examination, providing a clear and accurate visual representation of the membrane surface of the biomaterial composite.

2.2.2 Fourier Transform Infrared (FTIR)

Fourier Transform Infrared (FTIR) is a technique used to analyze interactions between molecules and infrared light [25]. This method finds the chemical bonds in a sample by looking at how the molecules in the sample absorb infrared radiation. The FTIR characterization can be performed using a PerkinElmer Frontier C90704 Spectrum IR Version 10.6.1. This instrument utilizes a Fourier transform interferometer to produce an infrared spectrum that encompasses information about molecular vibrations. The characterization process involves irradiating the sample with infrared light, where the chemical bonds in the sample absorb energy corresponding to their vibrations.

2.2.3 X-Ray Diffraction (XRD)

X-Ray Diffraction (XRD) is a scientific method that utilizes the interaction between X-rays and a crystal lattice to generate a diffraction pattern, which aids in the analysis of a substance's crystal structure [26]. The XRD used is the X'Pert PRO from PANalitycal MPD PW3040/60, which utilizes the diffraction properties of X-rays to unveil the crystal structure of the sample material. The wavelength of the X-ray tube with a Cu anode and a voltage of 40kV, with a current of 30mA, is scanned with a step size of 0.02° and a diffraction angle ranging from 10° to 90°.

2.2.4 Tensile test

Tensile testing is a method of determining the mechanical properties of a material or structure and its resistance to tensile or tension forces by measuring its ability to withstand these forces [27]. Tensile test can determine solid electrolyte membrane properties by testing strength and deformation under tension using standard ASTM D638 Type 5 with 20mm/minute.

2.2.5 Ion conductivity

The four NCC added membrane samples with compositions of 0g, 1g, 3g, and 5g underwent ionic conductivity testing by measuring their resistance values using a Corrtest 100E potentiostat utilizing Electrochemical Impedance Spectroscopy (EIS) with a potentiostatic frequency of 10 mHz

to 100 kHz, a DC voltage of 0 mV, and an AC voltage of 10 mVrms at room temperature and time. The stabilization process took approximately 10 minutes. The electrolyte's surface area was determined to be 4 square centimeters. The ionic conductivity of the samples was calculated using Eq. (1), after the stabilization process.

$$\sigma = \frac{L}{R.A} \text{ (S/cm)} \quad (1)$$

where, σ is the ionic conductivity, L is the thickness of the membrane, R is the resistance measured, and A is the surface area of the electrolyte. The above equation enables the determination of ionic conductivity through the resistance values obtained from electrochemical spectrometry tests. The results of this analysis offer important insights into the impact of NCC on the ionic conductivity of membranes, which can help improve their performance for a range of applications.

2.2.6 Impedance

Impedance is the resistance a circuit presents to the flow of alternating current (AC), denoted as |Z|. It is a complex quantity consisting of both resistance (Z_{re}) and reactance (Z_{im}). The Electrochemical Impedance Spectroscopy (EIS) was conducted under Potentiostatic conditions, with a frequency range of 10 mHz to 100 kHz. The applied voltage consisted of a direct current (DC) of 1 mV and an alternating current (AC) of 10 mVrms. The Z_{re} and Z_{im} values for each frequency will be recorded by the potentiostat during the EIS test. The impedance will then be calculated by taking the highest Z_{re} and Z_{im} value. Understanding impedance is crucial for analyzing electrical circuits, especially in AC circuits, as it influences how the circuit responds to different frequencies. This equation was used to compute the impedance. The impedance was calculated using Eq. (2):

$$|z| = \sqrt{(z_{re})^2 + (z_{im})^2} \text{ (Ohms)} \quad (2)$$

2.2.7 Cyclic voltametric

Cyclic voltammetry (CV) is a widely used and effective electrochemical method that is often used to study the reduction and oxidation reactions of molecular compounds [28]. CV is an electrochemical method that monitors the current as the electrode potential is raised and lowered in an electrolyte solution. An increase in potential causes oxidation, producing an anodic current, while a decrease in potential results in reduction and cathodic current. These current peaks provide information about redox reactions and the electrochemical properties of compounds in the electrolyte.

2.2.8 Power density

The parameter known as power density measures the amount of power generated or consumed per unit of time, volume, or area. The measure of power density, expressed in watts per centimeters square meter (W/cm^2), evaluates the efficiency of a system or device in converting or using energy. This statistic is typically presented in an official manner. The power of density was calculated using Eq. (3):

$$PD = \frac{E \cdot I}{A} \text{ (W/cm}^2\text{)} \quad (3)$$

where, PD refers to power density, while E represents voltage, I denotes current, and A signifies the surface area of the membranes.

2.3 Preparation of NCC paper

The manufacturing process of the NCC involves three distinct stages, namely pulping, bleaching, and hydrolysis. The pulping process refers to the procedure involved in the production of paper pulp. The paper is fragmented into smaller segments and subsequently subjected to milling processes. The paper was immersed in distilled water and then heated on a magnetic stirrer at 60°C for 2 hours using a 1.5% NaOH solution. This process aims to dissolve lignin and remove it from cellulose fibers, which leads to the production of more refined fibers. Following the completion of pulping, the subsequent stage involves the continuation of the bleaching process The bleaching process is a procedure used to achieve a whitening effect, which was conducted using a 3.5% sodium hypochlorite (NaClO). The paper pulp underwent dissolution through the utilization of a magnetic stirrer, operating at a temperature of 60°C, for a duration of 2 hours. The primary purpose of the bleaching process is to eliminate various substances that are responsible for imparting color, causing stains, or introducing contamination onto specific materials or substrates. After the completion of the bleaching procedure, the subsequent stage involves hydrolysis. The waste paper that had undergone processing was combined with a 400 ml solution of H_2SO_4, which had a concentration of 66%. For two hours, the mixture was stirred magnetically at a temperature of 45 degrees Celsius at a consistent rotational speed of 300 revolutions per minute. Then, the suspension liquid was centrifuged at 3000 r/min for 15 minutes, repeated iteratively until the pH became neutral [9].

2.4 Preparation of composite electrolyte membrane solution

A 4 g sample of polyvinyl alcohol (PVA) was ceased to exist in 100 mL of distilled water through the application of heat at approximately 80°C. The resulting solution was then subjected to magnetic stirring for a duration of 3 hours, during which time it achieved a state of clarity and homogeneity. A quantity of approximately 4 g of kalium hydroxide (KOH) was introduced into 20 milliliters of distilled water. The two solutions are combined. A sample of NCC was introduced into the PVA-KOH solution under constant and vigorous stirring at a speed of 300 revolutions per minute. Ensure that the mixture is thoroughly and uniformly mixed. Glycerol is introduced into the PVA/KOH/NCC mixture under continuous agitation and heating to ensure thorough homogenization of all constituents.

In determining membrane electrolyte composites for battery electrolytes, there are no specific standards. The primary criteria are that the composite must exhibit conductivity and the ability to store energy. The essential components of such a composite include a matrix, which provides the structural framework; reinforcement, which ensures mechanical strength and stability; and an electrolyte, which enables ion transport. As long as these components are present and the composite meets the necessary conductivity and energy storage requirements, it is deemed suitable for use in batteries.

3. RESULT AND DISCUSSION

3.1 Scanning electron microscopy (SEM) morphological

An analysis of SEM with a 3000-times magnitude at a scale of 50 micrometers was used to confirm the morphology of all membranes. The presented graph displays the SEM of four distinct samples: PVA/KOH/Glycerol (NCP0), PVA/KOH/Glycerol/1 g NCC paper (NCP1), PVA/KOH/Glycerol/3 g NCC paper (NCP3), and PVA/KOH/Glycerol/5 g of NCC paper (NCP5).

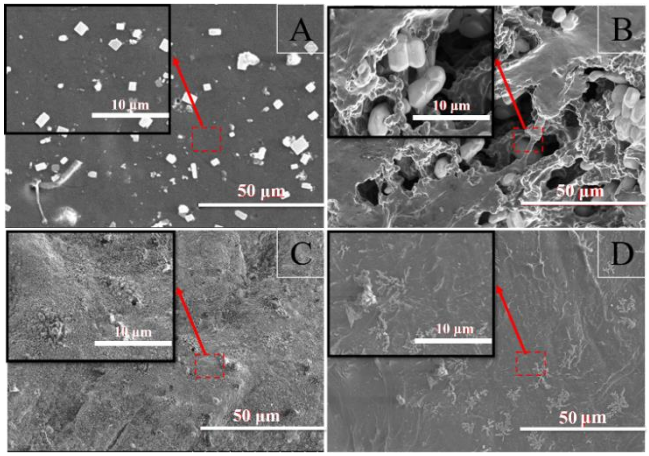

Figure 1. SEM with a magnification of 3000 times (a) NCP0, (b) NCP1, (c) NCP3, (d) NCP5

As shown in Figure 1(a), the surface morphology of the NCP0 sample had a uniform, rough, and homogeneous appearance. This indicates consistency in the structure, with the presence of a membranes that is smooth and homogeneous suggesting a high-quality coating that is evenly distributed throughout the membrane sample. This finding indicates that the addition of NCC paper did not result in any significant variation in the structure, resulting in a homogenous and cohesive appearance [29]. In Figure 1(b), NCP1 produces a slightly rough surface, but in some sample, it shows the presence of a mixture of NCC paper. This indicates there was a variation in the distribution and spread of NCC on the surface of the paper. In Figure 1(c), NCP3 produced a surface that was almost uniform, but almost completely covered the entire surface. This indicates a significant impact of the addition of NCC on the morphology of the membrane sample. Although the surface was almost uniform, the almost complete coverage of the entire surface indicated a more thorough dispersal of NCC, creating layers that involved a portion of the sample area [30]. In Figure 1(d), NCP5 produced a surface that was almost uniform and almost completely covered the entire surface. This indicates that the addition of NCC in a larger amount has a significant effect on the morphology of the membrane sample. The almost uniform surface and almost complete coverage indicate a more thorough dispersal of NCC, resulting in good quality coatings that are evenly distributed throughout the sample.

3.2 Fourier Transform Infrared (FTIR) analysis

Figure 2 displays the Fourier Transform Infrared (FTIR) spectra of four distinct samples. PVA has a wave length range of 3600-3200 cm^{-1}, 1800-1500 cm^{-1}, and 1300-1200 cm^{-1}, while KOH has a wave length range of 3600-3200 cm^{-1}, 1800-1500 cm^{-1}, and 1500-1350 cm^{-1} [31]. NCC has a range of 3600-3200 cm^{-1}, 3100-2900 cm^{-1}, and 1200-1000 cm^{-1} [9].

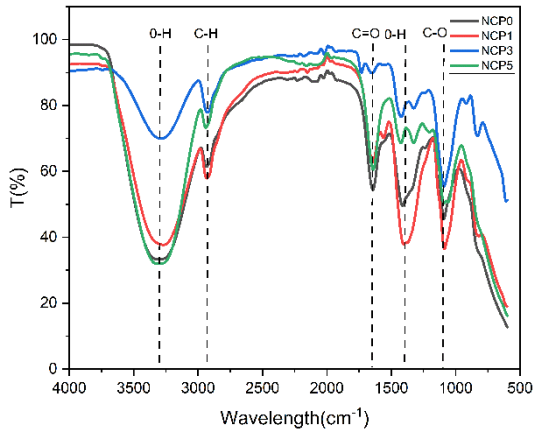

Figure 2. FTIR graph from the electrolyte membranes

The addition of NCC can affect absorption and transmission [32], with NCP3 indicating the highest increase in transmission. Variations in NCC concentration provide different effects on transmission. Higher concentration of NCC in NCP3 may cause an increase in transmission due to the enhanced functional group effect or better dispersion. However, at NCP5, a higher concentration may lead to changes, such as an increase in the penetration effect.

In the range of 3600-3200 cm^{-1}, the peaks in NCC can be associated with the O-H (hydroxyl) linkage [33]. This hydroxyl linkage involves the participation of hydroxyl groups from glucose in the cellulose matrix. The range of 3100-2900 cm^{-1} covers the peaks associated with the C-H (hydrogen carbon) linkage in organic compounds [34], including the C-H linkage in the carbon chain of glucose in the cellulose matrix [35]. The β-glucoside bond in NCC can be assigned to a specific range of infrared waves, namely approximately 1200-1000 cm^{-1}, which is known as the range of β-glucoside bond and reveals the atomic movements of oxygen and carbon atoms in the β-glucoside bond in the cellulose molecule [36].

3.3 X-Ray Diffraction (XRD) analysis

Table 1 and Figure 3 present the results of an experiment conducted to analyze crystallite size of electrolyte membranes.

Figure 3 illustrates the X-ray diffraction patterns of the various samples at different angles of incidence. The X-ray diffraction patterns of the samples exhibited varying degrees of intensity and position of the peaks with changes in the angle of incidence [37]. A comparison of the X-ray diffraction patterns of the different samples revealed that the peak positions underwent shifts as the angle of incidence was altered. The X-ray diffraction patterns of the samples were observed to change in response to changes in the angle of incidence. In Table 1, the XRD membrane displayed main peak positions at 7.7° on NCP0, 13.62° on NCP1, 10.05° on NCP3, and 11.52° on NCP5 [9]. These observations are presented in the appendix as a graph. In NCP0, a crystallite size of 83.5 nm was obtained. In NCP1, a crystallite size of 106.17 nm was obtained, in NCP3, a crystallite size of 128.28 nm was obtained, and in NCP5, a crystallite size of 119.2 nm was obtained. The crystallite size of NCP3 showed a significant change compared to the other samples.

Table 1. XRD of electrolyte membranes

Sample	Crystallite Size (nm)
PVA/KOH/Glycerol	83.5
PVA/KOH/Glycerol/1NCC	106.17
PVA/KOH/Glycerol/3NCC	128.28
PVA/KOH/Glycerol/5NCC	119.2

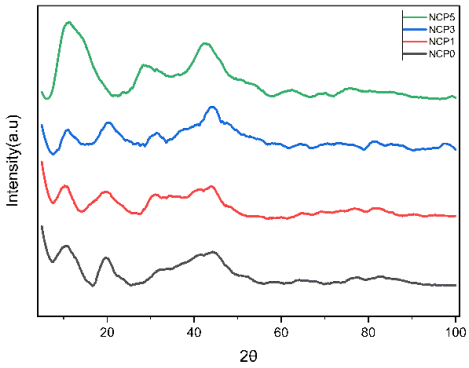

Figure 3. Graph XRD from electrolyte membranes

3.4 Tensile test

Figure 4 shows the tensile test on 4 electrolyte membrane samples. The results show that NCP0 has a tensile strength of 3.5 MPa with an elongation of 5.22 cm. NCP1 shows a tensile strength of 3.7 MPa with an elongation of 7.16 cm. NCP3 shows a tensile strength of 4.16 MPa with an elongation of 19.47 cm, and NCP5 shows a tensile strength of 6.91 MPa with an elongation of 12.06 cm.

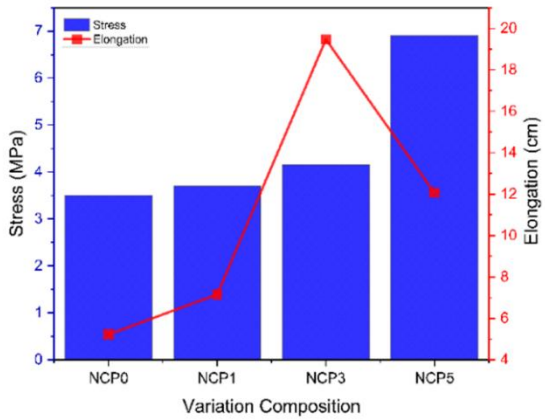

Figure 4. Graph tensile test of electrolyte membranes

Based on Figure 4, it is evident that NCP5 shows the greatest increase in tensile strength with a significant increase of 97.43%. However, the sample that showed the greatest elongation was NCP3 with a significant increase of 273.18%. These observations indicate that the incorporation of NCC at different concentrations has the potential to influence the mechanical characteristics of the specimen. NCP5 produces increased tensile strength, while NCP3 produces maximum elongation.

Although NCP5 has been observed to increase tensile strength, excessive amounts of NCC in the polymer matrix may result in increased stiffness of the structure. Therefore, in NCP3 the NCC particle distribution may show greater uniformity, resulting in a more elastic composite and consequently increased elongation.

3.5 Ionic conductivity

Figure 5 illustrates the membrane conductivity of NCP0, NCP1, NCP3, and NCP5. As shown in the sample graph, NCP3 shows a higher conductivity of 0.0512 S.cm-1 compared to the NCP0 membrane 0.0048 $S.cm^{-1}$ and NCP1 0.006 $S.cm^{-1}$. However, NCP5 has a lower conductivity than NCP3 with a value of 0.0456 $S.cm^{-1}$. This is because NCP3 is more dispersive than NCP5, resulting in a higher conductivity peak. On the other hand, NCP5 has a higher density than NCP3, making it more difficult for ions to move and reducing the conductivity value. Nevertheless, NCP5 has higher strength than other membranes due to the increased density of NCC paper.

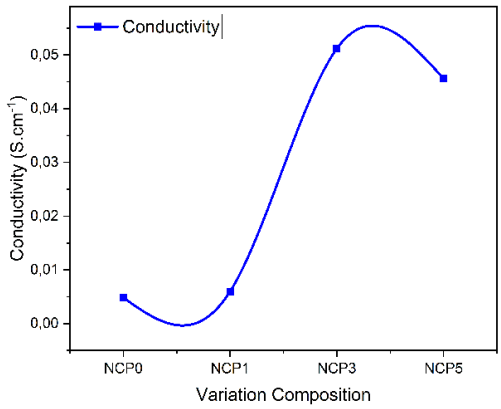

Figure 5. Graph conductivity of electrolyte membranes

3.6 Impedance

The impedance graph in Figure 6 will focus on two important aspects of impedance, namely the real component Z_{re} and the imaginary component Z_{im}.

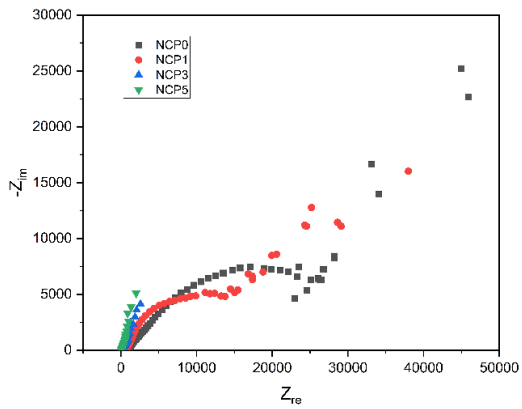

Figure 6. Graph impedance of electrolyte membranes

The partial impedance component exhibits the system's resistance or conductivity to a specific frequency current. If Zre increases, it may signify an augmentation in resistance or

a decrease in conductivity at that frequency. The imaginary impedance component reflects the capacitive or inductive response of a system. If Zim increases, it may suggest the presence of capacitive or inductive components in the system. Obtained from the enhanced NCC paper graph, it indicates an increased capacitance with the addition of NCC paper. The material matrix's properties, such as strength and elasticity, contribute to enhancing the overall conductivity. The incorporation of NCC paper can also heighten the capacitance of the membrane due to its impact on the arrangement of the material particles. This influence includes changes in the polarizability of the material and the interactions between dielectric particles, which can support the increase in capacitance. In the graph, the lowest impedance was obtained from sample NCP3, which was 4882.54 ohms. As the impedance decreases, the value of conductivity increases.

3.7 Cyclic voltametric

Figure 7 shows a voltametric cycle graph which shows the behavior of oxidation and reduction reactions at the anode, electrolyte and cathode.

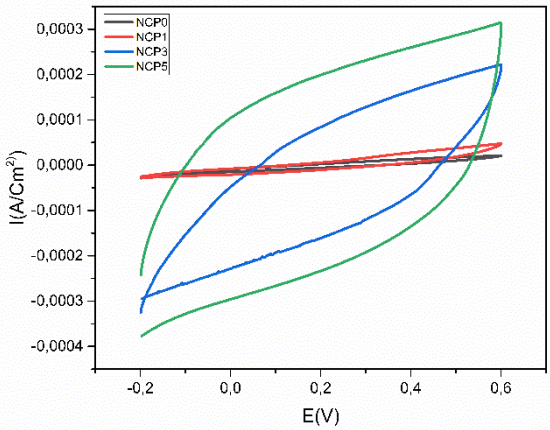

Figure 7. Cyclic 1 voltametric of electrolyte membranes

This graph shows the magnitude of the reduction and oxidation reaction peaks as well as the kinetics of electrochemical reactions by increasing and decreasing the voltage. NCP5 has a significant increase in power and exhibits higher electrochemical reaction intensity and thus has stronger reduction and oxidation reactions.

3.8 Power density

Table 2 presents the results of an experiment conducted to analyze power density of electrolyte membranes.

Table 2 shows the power density of adding NCC with variations of 0g, 1g, 3g, and 5g. There is a significant increase in power density with the inclusion of NCC in the system. NCP 5 has the largest increase in power density, namely 0.000188 W/cm^2. The significant increase in power density can be attributed to the contribution of NCC paper to the system conductivity and electrochemical properties. Positive results were seen in power density of NCP1, NCP3, and NCP5. Increasing the number of NCC appears to increase the power density capabilities of the system.

Table 2. Power density of electrolyte membrane

Sample	Power Density (W/cm^2)
PVA/KOH/Glycerol	1.27E-05
PVA/KOH/Glycerol/1NCC	2.85E-05
PVA/KOH/Glycerol/3NCC	1.33E-04
PVA/KOH/Glycerol/5NCC	1.88E-04

4. CONCLUSIONS

The study focuses on enhancing the ionic conductivity of electrolyte membranes by incorporating nanoparticles, specifically nanocrystalline cellulose (NCC). The addition of NCC to a PVA/KOH/Glycerol sample improved its tensile strength and ionic conductivity. NCP5 had the highest tensile strength (6.91 MPa) and conductivity (0.0456 S.cm^{-1}). NCP3 had the highest elongation (19.47 cm) and conductivity (0.0512 S.cm^{-1}). The incorporation of NCC also resulted in an increase in power density. These results suggest that NCC can enhance the mechanical and electrochemical properties of electrolyte membranes, making it a potential material for use in aluminum air batteries.

ACKNOWLEDGMENT

This research was supported by Andalas University, Indonesia through the Batch IV Indexed Publication Research Scheme, under Research Contract Number: 81/UN16.19/PT.01.03/IS-RPT/2023, during the fiscal year of 2023.

REFERENCES

[1] Gaele, M.F., Di Palma, T.M. (2022). Polymer electrolytes for Al-air batteries: Current state and future perspectives. Energy & Fuels, 36(21): 12875-12895. https://doi.org/10.1021/acs.energyfuels.2c02453

[2] Kumar, A., Ryparová, P., Hosseinpourpia, R., Adamopoulos, S., Prošek, Z., Žigon, J., Petrič, M. (2019). Hydrophobicity and resistance against microorganisms of heat and chemically crosslinked poly (vinyl alcohol) nanofibrous membranes. Chemical Engineering Journal, 360: 788-796. https://doi.org/10.1016/j.cej.2018.12.029

[3] Jamasri, F.Y., Yudhanto, F., Yudha, V., Syafri, E. (2023). Mechanical, physical and thermal characterization of PVA (Polyvinyl alcohol)/chitosan bioplastic film. International Journal of Heat and Technology, 41(3): 687-693. https://doi.org/10.18280/ijht.410322

[4] Du, E., Wang, Y., Sun, J., Yang, S. (2019). Experimental analysis on ductility of polyvinyl alcohol fibre reinforced concrete frame joints. In Annales de Chimie Science des Matériaux, 43(1): 17–22. https://doi.org/10.18280/acsm.430103

[5] Sapalidis, A.A. (2020). Porous Polyvinyl alcohol membranes: Preparation methods and applications. Symmetry, 12(6): 960. https://doi.org/10.3390/SYM12060960

[6] Wong, C.Y., Wong, W.Y., Loh, K.S., Daud, W.R.W., Lim, K.L., Khalid, M., Walvekar, R. (2020). Development of poly (vinyl alcohol)-based polymers as proton exchange membranes and challenges in fuel cell application: A review. Polymer Reviews, 60(1): 171-202.

https://doi.org/10.1080/15583724.2019.1641514
[7] Li, Y., Zhou, W., Zhou, P., Zhou, Z. (2022). Properties and application progress of nano cellulose. In Second International Conference on Medical Imaging and Additive Manufacturing (ICMIAM 2022), 12179: 194-198. https://doi.org/10.1117/12.2637386
[8] Hatta, F.F., Yahya, M.Z.A., Ali, A.M.M., Subban, R.H.Y., Harun, M.K., Mohamad, A.A. (2005). Electrical conductivity studies on PVA/PVP-KOH alkaline solid polymer blend electrolyte. Ionics, 11: 418-422. https://doi.org/10.1007/BF02430259
[9] Zhang, X., Li, S., Li, J., Fu, B., Di, J., Xu, L., Zhu, X. (2021). Reinforcing effect of nanocrystalline cellulose and office waste paper fibers on mechanical and thermal properties of poly (lactic acid) composites. Journal of Applied Polymer Science, 138(21): 50462. https://doi.org/10.1002/app.50462
[10] Orue, A., Santamaria-Echart, A., Eceiza, A., Peña-Rodriguez, C., Arbelaiz, A. (2017). Office waste paper as cellulose nanocrystal source. Journal of Applied Polymer Science, 134(35): 45257. https://doi.org/10.1002/app.45257
[11] Wang, X., Yao, C., Wang, F., Li, Z. (2017). Cellulose-based nanomaterials for energy applications. Small, 13(42): 1702240. https://doi.org/10.1002/smll.201702240
[12] Muhd Julkapli, N., Bagheri, S. (2017). Nanocellulose as a green and sustainable emerging material in energy applications: A review. Polymers for Advanced Technologies, 28(12): 1583-1594. https://doi.org/10.1002/pat.4074
[13] Yang, Y., Chen, Z., Zhang, J., Wang, G., Zhang, R., Suo, D. (2019). Preparation and applications of the cellulose nanocrystal. International Journal of Polymer Science, 2019(1): 1767028. https://doi.org/10.1155/2019/1767028
[14] Udomluck, N., Koh, W.G., Lim, D.J., Park, H. (2019). Recent developments in nanofiber fabrication and modification for bone tissue engineering. International Journal of Molecular Sciences, 21(1): 99. https://doi.org/10.3390/ijms21010099
[15] Sazali, N., Mamat, R., Siregar, J.P., Gunawan, T., Salleh, W.N.W., Nordin, N.A.H.M. (2020). PI/NCC carbon membrane: Effect of additives loading towards hydrogen separation. In IOP Conference Series: Materials Science and Engineering, 736(2): 022002. https://doi.org/10.1088/1757-899X/736/2/022002
[16] Rezeikinta, F.A., Kasim, A., Syafri, E., Chaniago, I., Ridwan, F. (2023). Reducing water absorption and increasing the density of kapok (Ceiba pentandra, L.) fibers from kapok production center in Indonesia. International Journal of Design & Nature and Ecodynamics, 18(1): 195–200. https://doi.org/10.18280/ijdne.180124
[17] Bangar, S.P., Whiteside, W.S. (2021). Nano-cellulose reinforced starch bio composite films-A review on green composites. International Journal of Biological Macromolecules, 185: 849-860. https://doi.org/10.1016/j.ijbiomac.2021.07.017
[18] Rochardjo, H.S., Fatkhurrohman, A.K., Yudhanto, F. (2021). Fabrication of nanofiltration membrane based on polyvinyl alcohol nanofibers reinforced with cellulose nanocrystal using electrospinning techniques. International Journal of Technology (IJTech), 12(2): 329-338. https://doi.org/10.14716/ijtech.v12i2.4173
[19] Aziz, S.B., Asnawi, A.S., Abdulwahid, R.T., Ghareeb, H.O., Alshehri, S.M., Ahamad, T., Hadi, J.M., Kadir, M.F.Z. (2021). Design of potassium ion conducting PVA based polymer electrolyte with improved ion transport properties for EDLC device application. Journal of Materials Research and Technology, 13: 933-946. https://doi.org/10.1016/j.jmrt.2021.05.017
[20] Yuan, A., Zhao, J. (2006). Composite alkaline polymer electrolytes and its application to nickel–metal hydride batteries. Electrochimica acta, 51(12): 2454-2462. https://doi.org/10.1016/j.electacta.2005.07.027
[21] Hatta, F.F., Kudin, T.I.T., Subban, R.H.Y., Ali, A.M.M., Harun, M.K., Yahya, M.Z.A. (2009). Plasticized PVA/PVP–KOH alkaline solid polymer blend electrolyte for electrochemical cells. Functional Materials Letters, 2(03): 121-125. https://doi.org/10.1142/S179360470900065X
[22] Bilck, A.P., Müller, C.M.O., Olivato, J.B., Mali, S., Grossmann, M.V.E., Yamashita, F. (2015). Using glycerol produced from biodiesel as a plasticiser in extruded biodegradable films. Polímeros, 25(4): 331-335. https://doi.org/10.1590/0104-1428.1803
[23] Suarez Palacios, O.Y., Narvaez Rincon, P.C., Corriou, J.P., Camargo Pardo, M., Fonteix, C. (2014). Low-molecular-weight glycerol esters as plasticizers for poly (vinyl chloride). Journal of Vinyl and Additive Technology, 20(2): 65-71. https://doi.org/10.1002/vnl.21351
[24] Inkson, B.J. (2016). Scanning electron microscopy (SEM) and transmission electron microscopy (TEM) for materials characterization. In Materials characterization using nondestructive evaluation (NDE) methods, pp. 17-43. https://doi.org/10.1016/B978-0-08-100040-3.00002-X
[25] Dutta, A. (2017). Fourier transform infrared spectroscopy. Spectroscopic Methods for Nanomaterials Characterization, 73-93. https://doi.org/10.1016/c2009-0-22072-1
[26] Bunaciu, A.A., UdriŞTioiu, E.G., Aboul-Enein, H.Y. (2015). X-ray diffraction: Instrumentation and applications. Critical Reviews in Analytical Chemistry, 45(4): 289-299. https://doi.org/10.1080/10408347.2014.949616
[27] Yalcin, D. (2021). Tensile testing concepts & definitions. ResearchGate, pp. 1–12.
[28] Elgrishi, N., Rountree, K.J., McCarthy, B.D., Rountree, E.S., Eisenhart, T.T., Dempsey, J.L. (2018). A practical beginner's guide to cyclic voltammetry. Journal of Chemical Education, 95(2): 197-206. https://doi.org/10.1021/acs.jchemed.7b00361
[29] Jahan, Z., Niazi, M.B.K., Gregersen, Ø.W. (2018). Mechanical, thermal and swelling properties of cellulose nanocrystals/PVA nanocomposites membranes. Journal of Industrial and Engineering Chemistry, 57: 113-124. https://doi.org/10.1016/j.jiec.2017.08.014
[30] Chen, S., Chen, M., Huang, H., Liu, X., Qu, B., Wang, R., Liu, K.W., Zheng, Y.Y., Zhuo, D. (2022). Nanocrystalline cellulose–and graphene oxide–reinforced polyvinyl alcohol films: Synthesis, characterization, and origin of beneficial co-filling effects. Applied Composite Materials, 29(4): 1597-1619. https://doi.org/10.1007/s10443-022-10033-4
[31] Almafie, M.R., Nawawi, Z., Jauhari, J., Sriyanti, I.

(2020). Electrospun of Poly (vinyl alcohol)/Potassium hydroxide (PVA/KOH) nanofiber composites using the electrospinning method. In IOP Conference Series: Materials Science and Engineering, 850(1): 012051. https://doi.org/10.1088/1757-899X/850/1/012051

[32] Liu, J., Li, Y., Jin, C., Lin, H., Li, H., Shen, J. (2023). Preparation and mechanism analysis of nanocrystalline cellulose-tricalcium silicate paste composite with high electromagnetic transmission performance. Cement and Concrete Composites, 143: 105233. https://doi.org/10.1016/j.cemconcomp.2023.105233

[33] Beneventi, P., Capelletti, R., Kovács, L., Péter, A., Manotti, A.L., Ugozzoli, F. (1994). FTIR spectroscopy of OH stretching modes in BSO, BGO and BTO sillenites. Journal of Physics: Condensed Matter, 6(31): 6329. https://doi.org/10.1088/0953-8984/6/31/032

[34] Syarifuddin, S. H., Hayatun, A., Ahmad, A., Taba, P., Fauziah, S., Sondari, D., Karim, H., Irfandi, R. (2023). Synthesis and its application as packaging of bioplastic from rice huck cellulose citrate using chitosan and sorbitol plasticizers. Int. J. Des. Nat. Ecodynamics, 18(2): 435–441. https://doi.org/10.18280/ijdne.180222

[35] Barrios, V.A.E., Méndez, J.R.R., Aguilar, N.V.P., Espinosa, G.A., Rodríguez, J.L.D. (2012). FTIR-an essential characterization technique for polymeric materials (Vol. 4). InTech. https://doi.org/10.5772/36044

[36] Spiridon, I., Teacă, C.A., Bodîrlău, R. (2011). Pretreatment with ionic liquids. BioResources, 6(1): 400–413.

[37] Ali, A., Chiang, Y.W., Santos, R.M. (2022). X-ray diffraction techniques for mineral characterization: A review for engineers of the fundamentals, applications, and research directions. Minerals, 12(2): 205. https://doi.org/10.3390/min12020205

NOMENCLATURE

σ	ionic conductivity, $S.cm^{-1}$
Z	impedance, ohm
Z_{re}	resistance, ohm
Z_{im}	reactance, ohm
PD	power density, $W.m^{-2}$
wv	wavelength, cm^{-1}
cs	crystallite size, nm